Available online at www.sciencedirect.com
ScienceDirect
Journal of Sound and Vibration 310 (2008) 433–441
JOURNAL OF SOUND AND VIBRATION
www.elsevier.com/locate/jsvi

Short Communication

Large deflections and vibration of a tapered cantilever pulled at its tip by a cable ☆

David B. Holland[a], Lawrence N. Virgin[a,*], Raymond H. Plaut[b]

[a]School of Engineering, Duke University, Durham, NC 27708-0300, USA
[b]Department of Civil and Environmental Engineering, Virginia Polytechnic Institute and State University, Blacksburg, VA 24061, USA

Received 6 April 2006; received in revised form 2 October 2006; accepted 27 June 2007
Available online 14 September 2007

Abstract

The behavior of a slender, tapered, cantilever beam loaded through a cable attached to its free end is described. Large static deflections are computed (based on an elastica description) together with natural frequencies and mode shapes for small-amplitude vibrations about equilibrium. Experimental results exhibit good agreement with the theoretical results.

1. Introduction

Square, kite-shaped solar-sails utilize highly flexible booms that may buckle. These buckled booms may be used to impart tension into a solar sail membrane. A related problem is the behavior of a cantilever pulled at its tip by a cable. The other end of the cable is assumed to be located near the fixed end of the cantilever, and a device such as a turnbuckle is used to shorten the cable. Deformation of the beam occurs as soon as the ends of the cable move toward each other. The deflections become large as the cable is shortened. These equilibrium shapes are investigated, as well as small vibrations about equilibrium.

Critical loads for a cantilever subjected to a load that passes through its base or another point on the original axis of the beam were presented by Timoshenko and Gere [1] and verified experimentally by Willems [2]. Vibrations about the straight prebuckled equilibrium configuration were examined by Huang et al. [3], Anderson and Done [4], Sugiyama et al. [5], and Xiong et al. [6]. Mladenov and Sugiyama [7] investigated postbuckled equilibrium shapes.

Here, the cable does not pass through a specific point along the beam's axis, but ends at a point that is slightly offset from the beam's base. The problem does not involve a critical load (or critical shortening of the cable) at which the beam departs from a straight shape. Instead, as the cable is shortened, the beam bends. This problem was studied by Holland et al. [8] in the case of a prismatic beam (i.e., with constant bending stiffness with respect to the plane of buckling). It may be advantageous to vary the cross-section of the beam

☆This paper was presented at the Ninth International Conference on Recent Advances in Structural Dynamics, Southampton, July 2006.

*Corresponding author. Tel.: +1 919 660 5342; fax: +1 919 660 5219.
E-mail address: l.virgin@duke.edu (L.N. Virgin).

0022-460X/$ - see front matter © 2007 Published by Elsevier Ltd.
doi:10.1016/j.jsv.2007.06.075

along its length, such as for the purpose of reducing the weight, which should be as low as possible for applications in space. It is assumed in this paper that the width of the beam decreases linearly from the beam's base to its tip. Deflections and vibrations are investigated.

A few studies involving buckled beams will be mentioned. Buckling loads for tapered beams were examined in Refs. [1,9,10], among others. Postbuckling was considered in Refs. [11–13]. Salter [14] conducted experiments on steel beams. Finally, vibrations were investigated in [15,16].

An analysis of the problem under consideration is described in the next section. In subsequent sections, the experimental procedure is presented, followed by results and concluding remarks.

2. Analytical formulation

The beam is shown in Figs. 1 and 2. It is linearly elastic with modulus of elasticity E, density ρ, and length L, and is modeled as an inextensible elastica. Gravitational effects and damping are neglected. Two-dimensional deflections in the $x-y$ plane are considered. The coordinates of points on the beam are $x(s,t)$ and $y(s,t)$, where s is the arc length and t is time. The rotation is $\theta(s,t)$. The depth of the cross-section is

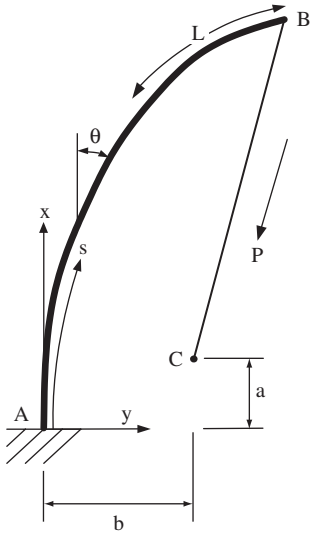

Fig. 1. Geometry of beam-cable system.

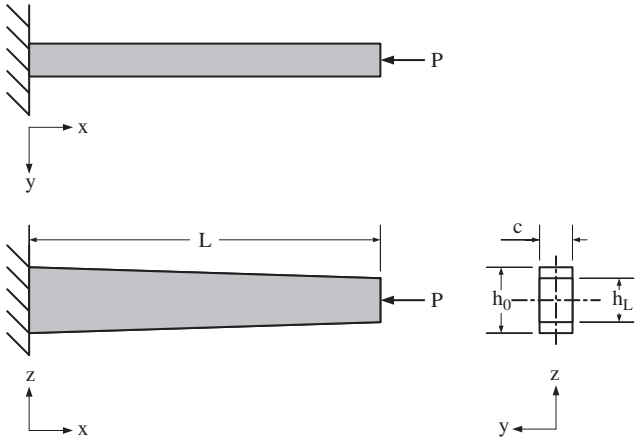

Fig. 2. Cantilever with rectangular cross-section of constant depth and linearly tapered width.

c, and the width of the cross-section decreases linearly from h_0 at $s = 0$ to h_L at $s = L$. The taper ratio is defined as $\alpha = h_L/h_0$, so that $\alpha = 1$ for the prismatic case. The mass per unit length $m(s)$ and the bending stiffness $EI(s)$ with respect to the plane of buckling are both proportional to the width $h(s)$, and hence their ratio $m(s)/(EI(s))$ is constant.

As depicted in Fig. 1, the cable connects point B, the tip of the beam, with point C, where $(x, y) = (a, b)$. The bending moment in the beam is $M(s, t)$, and the internal force has components $P_v(s, t)$ and $P_h(s, t)$ parallel to the $-x$ and $-y$ axes on a positive face, respectively. Therefore the cable tension $P(t)$ has components $P_v(L, t)$ and $P_h(L, t)$. From geometry, the moment–curvature relation, and dynamic equilibrium, the governing equations for the beam are:

$$\begin{aligned} &\partial x/\partial s = \cos\theta, \quad \partial y/\partial s = \sin\theta, \\ &\partial\theta/\partial s = M/EI, \quad \partial M/\partial s = P_h\cos\theta - P_v\sin\theta, \\ &\partial P_v/\partial s = -m\,\partial^2 x/\partial t^2, \quad \partial P_h/\partial s = -m\,\partial^2 y/\partial t^2. \end{aligned} \tag{1}$$

The boundary conditions are $x(0, t) = 0$, $y(0, t) = 0$, $\theta(0, t) = 0$, $M(L, t) = 0$, $[y(L, t) - b]P_v(L, t) = [x(L, t) - a]P_h(L, t)$.

The subscripts e and d are used to denote equilibrium and dynamic quantities, respectively. The equilibrium equations are:

$$\begin{aligned} &\mathrm{d}x_e/\mathrm{d}s = \cos\theta_e, \quad \mathrm{d}y_e/\mathrm{d}s = \sin\theta_e, \\ &\mathrm{d}\theta_e/\mathrm{d}s = M_e/EI, \quad \mathrm{d}M_e/\mathrm{d}s = P_{\mathrm{he}}\cos\theta_e - P_{\mathrm{ve}}\sin\theta_e, \end{aligned} \tag{2}$$

where P_{he} and P_{ve} are constant. The dynamic quantities are small and have frequency ω. They are governed by the linear equations

$$\begin{aligned} &\mathrm{d}x_d/\mathrm{d}s = -\theta_d\sin\theta_e, \quad \mathrm{d}y_d/\mathrm{d}s = \theta_d\cos\theta_e, \\ &\mathrm{d}\theta_d/\mathrm{d}s = M_d/EI, \quad \mathrm{d}M_d/\mathrm{d}s = P_{\mathrm{hd}}\cos\theta_e - P_{\mathrm{vd}}\sin\theta_e - \theta_d(P_{\mathrm{he}}\sin\theta_e + P_{\mathrm{ve}}\cos\theta_e), \\ &\mathrm{d}P_{\mathrm{hd}}/\mathrm{d}s = m\omega^2 x_d, \quad \mathrm{d}P_{vd}/\mathrm{d}s = m\omega^2 y_d. \end{aligned} \tag{3}$$

The boundary conditions are obtained from the ones listed above, as well as the assumption that the cable is linearly elastic and acts like a spring with stiffness k [8].

Numerical solutions for equilibrium and then for vibration are obtained with the use of shooting methods in Matlab [17]. The quantities a, b, L, E, ρ, c, h_0, h_L, and k are specified, and the unknown parameters and conditions at $s = 0$ are varied until the known conditions at $s = L$ are satisfied with sufficient accuracy.

3. Experiments

Experiments were performed on linearly tapered polycarbonate beams. The set-up consisted of a beam sample clamped between two steel plates, and mounted to a small-amplitude (4 mm) dynamic shaker. A steel cable with an approximate length of 711 mm, diameter of 0.46 mm, and axial stiffness of $k = 12.4\,\mathrm{N/mm}$ was attached to the free end of the beam. The cable was connected to a small turnbuckle, which was attached to a load cell that could be moved to different offsets from the base of the beam. A photographic image of the test set-up is shown in Fig. 3.

Five different beam shapes were tested, with $L = 737\,\mathrm{mm}$, $c = 4.67\,\mathrm{mm}$, $E = 1.8\,\mathrm{GPa}$, $\rho g = 1113\,\mathrm{kg/m^3}$, $h_0 = 31.72\,\mathrm{mm}$, and $h_L = 6.35, 12.7, 19.05, 25.4$, and $31.75\,\mathrm{mm}$ (i.e., taper ratios $\alpha = 0.2, 0.4, 0.6, 0.8$, and 1.0). The end C of the cable in Fig. 1 was placed with $a = 28.575\,\mathrm{mm}$ (i.e., $a/L = 0.0388$) and four different values of b: 15.875, 25.4, 38.1, and 50.8 mm (i.e., $b/L = 0.0216, 0.0345, 0.0517$, and 0.069).

A reflective target point was selected near the end of the beam to gather velocity information during the dynamic measurements. An accelerometer mounted on the clamping plates was used to measure the acceleration at the base of the beam. The acceleration was numerically integrated by the data acquisition system to provide the velocity input to the system. The shaker was used to excite the system with bandlimited random noise (1–100 Hz). This frequency region contains the first four natural frequencies of the system. The frequency response relating the velocity at the base (the input) to the velocity near the end of the beam

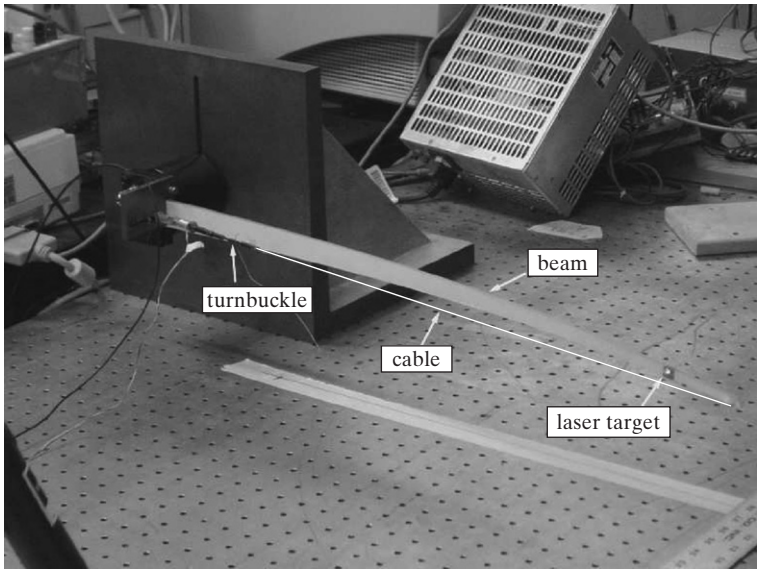

Fig. 3. The experimental configuration.

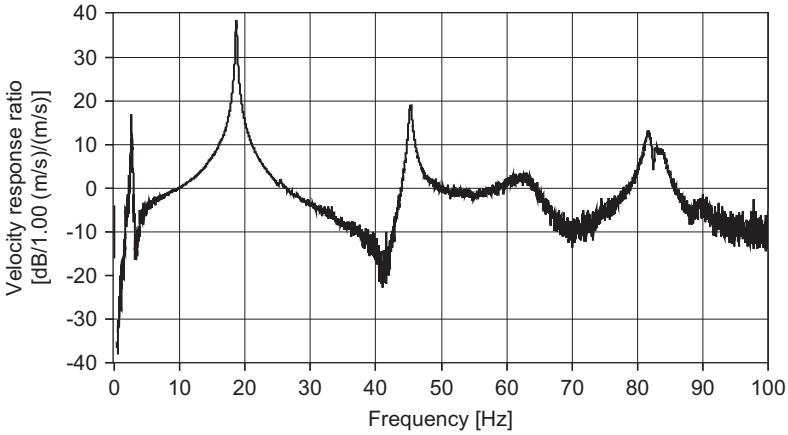

Fig. 4. Sample frequency-response plot from experiments.

(the output) was estimated for each applied cable tension level. The H_3 frequency response estimate was calculated using the input velocity power spectral density, the output velocity power spectral density, and the velocity cross-spectral density between the input and output signals. Each spectral density estimate was derived from 10 discrete Fourier transforms of 8 s duration segments of sampled input and output data, each windowed with a Hanning window. The overlap between segments was 66%. A sample frequency-response plot is shown in Fig. 4, with the abscissa in Hz and the ordinate in dB.

4. Results

The material and geometric parameters from the experiments are also used in the numerical analysis. Thus only the transverse offset b, taper ratio α, and cable tension P need to be listed in the results presented in this section.

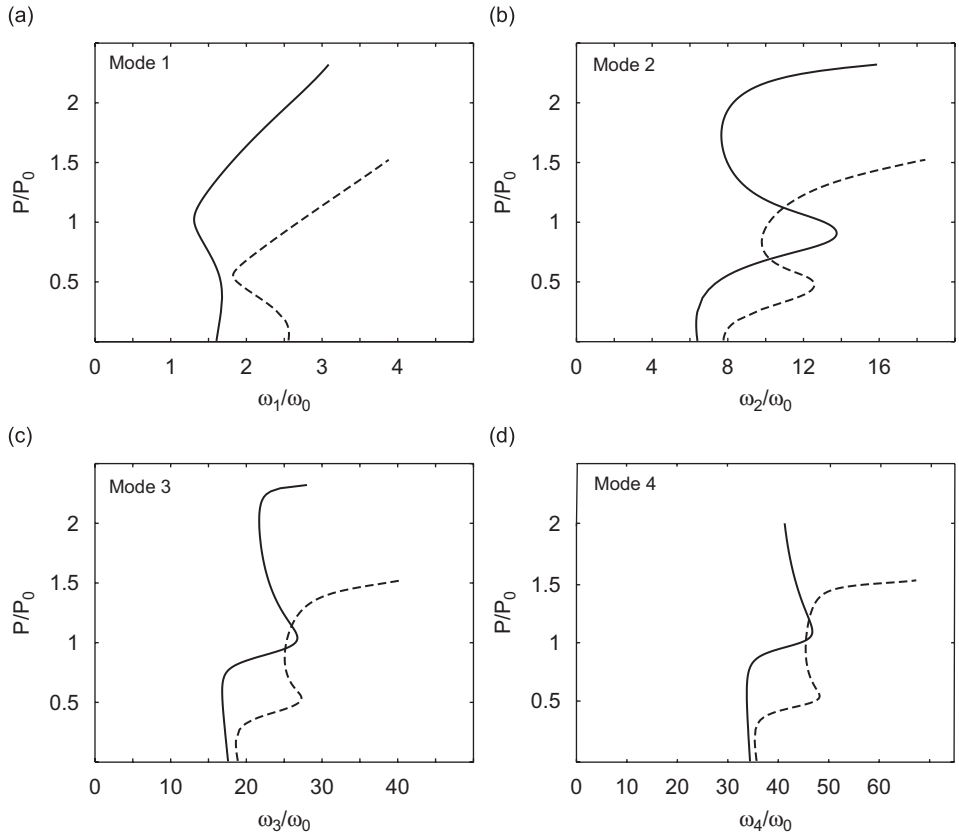

Fig. 5. Variation of first four vibration frequencies with cable tension for prismatic beam ($\alpha = 1$, continuous line) and for tapered beam ($\alpha = 0.2$, dashed line) when $b/L = 0.0216$.

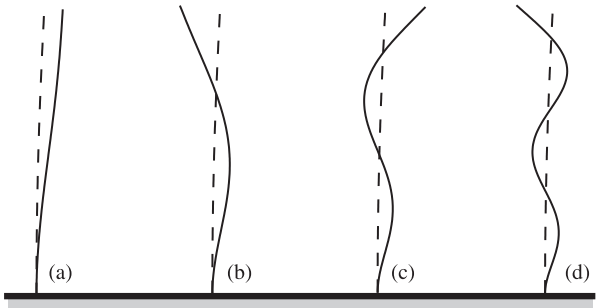

Fig. 6. Mode shapes from numerical analysis when $b/L = 0.0216$, $\alpha = 0.2$, and $P = 2.71$ N: (a) first mode, (b) second mode, (c) third mode, (d) fourth mode. The dashed line indicates the equilibrium position.

The relationships between the cable tension P and the first four vibration frequencies (ω_n, $n = 1, 2, 3, 4$) are shown in Fig. 5 for the prismatic beam and the tapered beam with $\alpha = 0.2$ when $b/L = 0.0216$. The cable tension P is normalized by the critical load P_0 for the prismatic beam with no offset ($P_0 = \pi^2 EI/(L^2) = 8.76$ N) and each frequency ω_n is normalized by the fundamental frequency ω_0 of the prismatic beam under no load ($\omega_0 = 3.516(EI)^{1/2}(\rho h_0 c L^4)^{-1/2} = 11.1$ rad/s). As the cable is tightened, the first (fundamental) frequency tends to decrease as P approaches its critical value for the case of no offset (i.e., if $a/L = b/L = 0$), and then to

increase as P is increased further. The other three frequencies in Fig. 5 tend to behave oppositely near the critical load, increasing and then decreasing. Then they tend to increase again as the load passes another threshold.

Fig. 6 depicts the equilibrium shape and the first four mode shapes obtained numerically when $b/L = 0.0216$, $\alpha = 0.2$, and $P = 2.713\,\mathrm{N}$. Only small vibrations about equilibrium are analyzed, but the amplitudes are magnified in Fig. 6 so the modes can be clearly seen. The nth vibration mode has $n-1$ internal nodes. In these mode shapes, the largest deflection occurs at the tip of the beam.

The effects of the cable tension on the transverse tip deflection (in equilibrium) and the first four vibration frequencies are depicted in Figs. 7 and 8 for taper ratios $\alpha = 0.8$ and 0.2, respectively. The tip deflection $y_e(L)$ is normalized by the beam length $L = 737\,\mathrm{mm}$. Numerical solutions are depicted by solid curves. Circles denote mean values of the experimental results, with possible errors of approximately 5%. The numerical and experimental results exhibit good agreement.

As the taper ratio α decreases, the amount of material decreases and the zero offset critical load decreases (i.e., it is equal to 7.87, 6.94, 5.96, and 4.85 N, respectively, for $\alpha = 0.8, 0.6, 0.4$, and 0.2). Hence the first frequency veers toward smaller values, and the next three frequencies veer toward larger values at a lower load in Fig. 8 than in Fig. 7. The mass and bending stiffness of the beam both decrease as α decreases, and these effects tend to counteract each other, so the frequencies tend to be in similar ranges in Figs. 7 and 8. The load at which the tip deflection has a relative maximum in Fig. 8 is lower than in Fig. 7.

Moving the cable's lateral attachment point away from the beam (i.e., increasing b/L) may be interpreted as increasing the amplitude of an imperfection. In the equilibrium plots, the slope of the initial part of the curve decreases as b/L increases. The load for which the tip deflection has a relative maximum in Fig. 7 is almost the same for the four values of b/L, and a similar property holds in Fig. 8.

5. Concluding remarks

A thin cantilevered beam, compressed by a cable attached to the tip and terminating near the base, was considered. This system is related to solar-sail structures in which a structural boom bends in order to put the sail membrane under tension. In the analytical part of the study, a shooting method was used to obtain numerical solutions for the equilibrium shapes (including large deflections) and for small vibrations about equilibrium. In the experimental part of the study, a polycarbonate strip was bent by a cable that was tightened with a turnbuckle. Four different cable attachment points near the beam's base were considered. The first four frequencies and mode shapes were determined.

The width of the beam was tapered linearly. Four different amounts of taper were examined, along with the case of a prismatic beam. Results from the experiments were close to those from the numerical procedure based on an inextensible elastica and a linearly elastic cable with no inertia or bending.

Due to the offset of the cable attachment from the base of the beam, the problem does not involve buckling of a straight member loaded axially. Instead, the beam deflects as soon as the cable is tightened, like a column with an imperfection. The tip of the beam moves away from the original axis, and after a certain threshold tension the tip moves toward the axis. Also, as the cable tension is increased from zero, the first frequency initially decreases and then increases. The next three frequencies tend to increase initially (although the third and fourth frequency may exhibit very little change for sufficiently small tensions), then decrease, and then increase again as the cable tension becomes large and the beam becomes severely bent.

Results were presented for taper ratios $\alpha = 0.8$ and 0.2, where α is the ratio of the width of the beam at the tip to that at the base. Further results for $\alpha = 1$ (prismatic beam), 0.6, and 0.4 can be found in Ref. [18]. As the cable is tightened, the lateral tip deflection is larger if α is smaller (i.e., if the taper angle is larger and the beam has less material). The general behavior of the frequencies as the tension is increased is similar for different taper ratios. Lateral offsets of the fixed end of the cable ranged up to $0.069\,L$, where L is the beam length. With larger offset, the initial deflections increased, but again the forms of the tension-frequency plots of the first four frequencies did not change significantly.

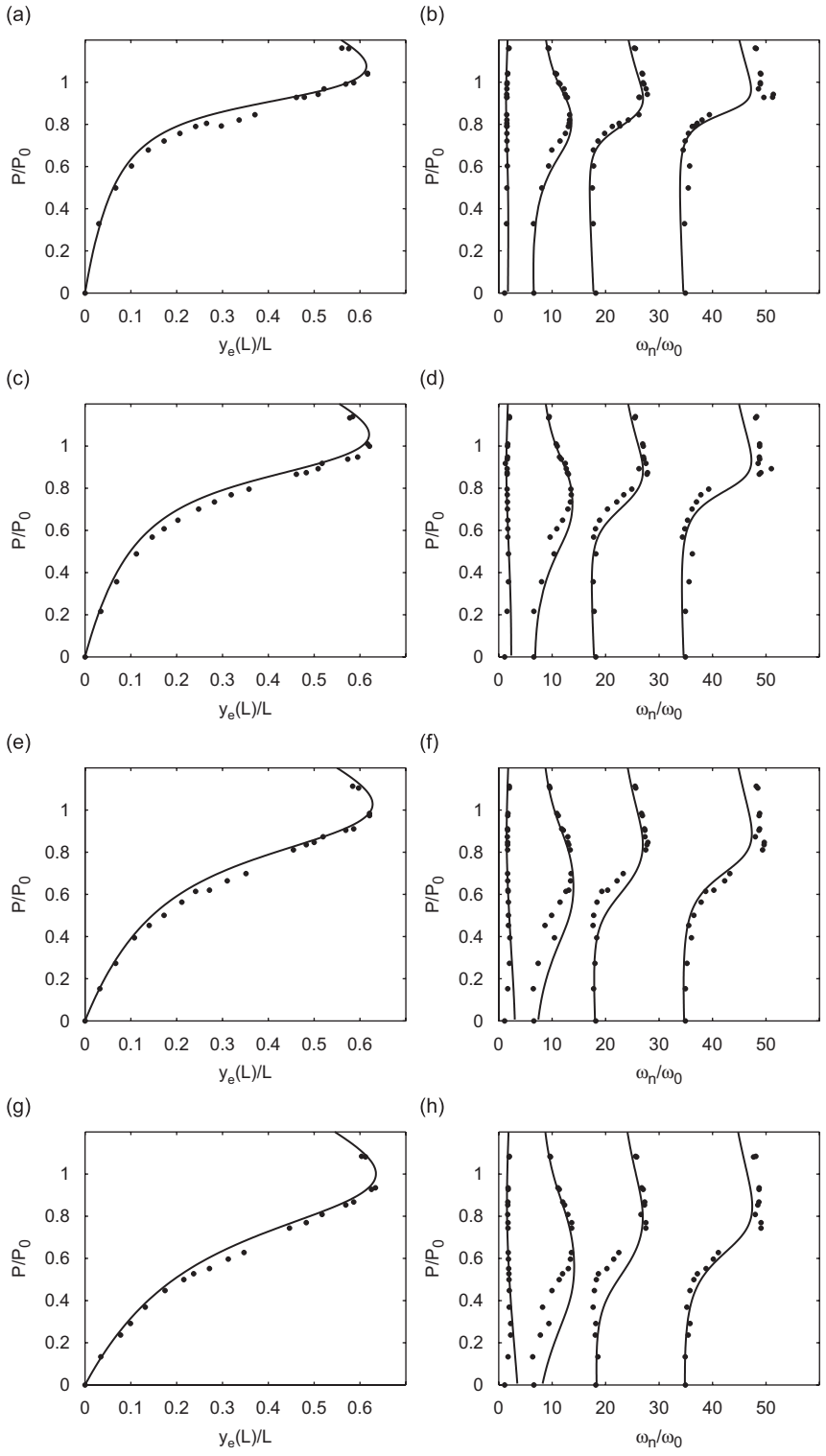

Fig. 7. Equilibrium plots (normalized cable tension versus normalized transverse tip deflection), and variation of first four normalized vibration frequencies with normalized cable tension, for $\alpha = 0.8$ and $b/L = 0.0216$ (parts (a) and (b)), 0.0345 (parts (c) and (d)), 0.0517 (parts (e) and (f)), and 0.069 (parts (g) and (h)). Circles represent experimental results.

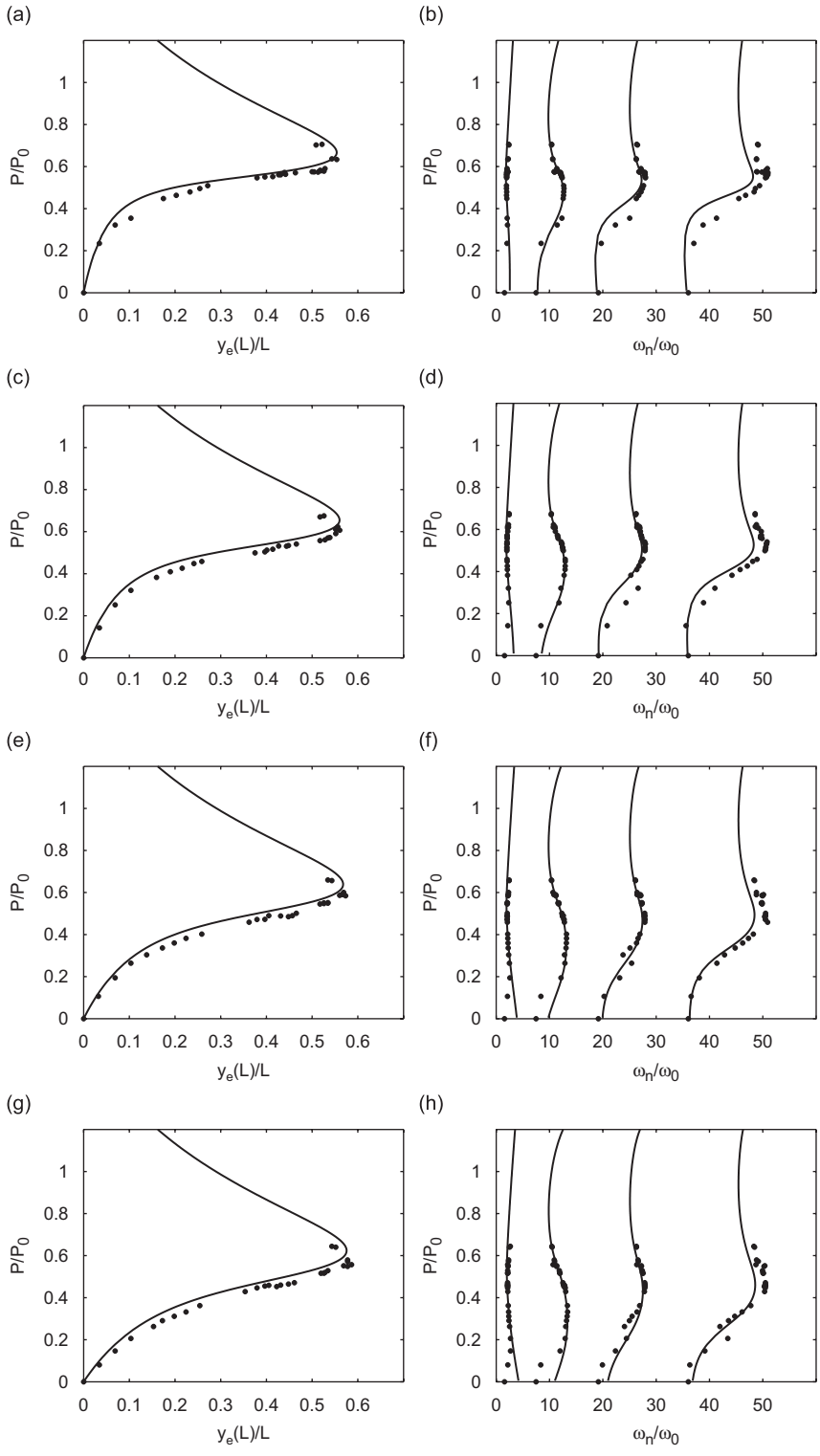

Fig. 8. Equilibrium plots (normalized cable tension versus normalized transverse tip deflection), and variation of first four normalized vibration frequencies with normalized cable tension, for $\alpha = 0.2$ and $b/L = 0.0216$ (parts (a) and (b)), 0.0345 (parts (c) and (d)), 0.0517 (parts (e) and (f)), and 0.069 (parts (g) and (h)). Circles represent experimental results.

Acknowledgments

The first author acknowledges the support of the *NASA Graduate Student Research Program* (*GSRP*). The third author acknowledges the support of the *National Science Foundation* under Grant 0114709.

References

[1] S.P. Timoshenko, J.M. Gere, *Theory of Elastic Stability*, second ed., McGraw-Hill, New York, 1961.
[2] N. Willems, Experimental verification of the dynamic stability of a tangentially loaded cantilever column, *Journal of Applied Mechanics* 33 (1966) 460–461.
[3] N.C. Huang, W. Nachbar, S. Nemat-Nasser, On Willems' experimental verification of the critical load in Beck's problem, *Journal of Applied Mechanics* 34 (1967) 243–245.
[4] N.A. Anderson, G.T.S. Done, On the partial simulation of a nonconservative system by a conservative system, *International Journal of Solids and Structures* 7 (1971) 183–191.
[5] Y. Sugiyama, K.A. Mladenov, K. Fusayasu, *Stability and vibration of elastic systems subjected to a central force, Reports 14/1*, Faculty of Engineering, Tottori University, Japan, 1983.
[6] Y. Xiong, T.K. Wang, B. Tabarrok, On a centripetally loaded model simulating Beck's column, *International Journal of Solids and Structures* 25 (1989) 1107–1113.
[7] K.A. Mladenov, Y. Sugiyama, Buckling of elastic cantilevers subjected to a polar force: exact solution, *Transactions of the Japanese Society for Aeronautical Space Sciences* 26 (1983) 80–90.
[8] D.B. Holland, I. Stanciulescu, L.N. Virgin, R.H. Plaut, Vibration and large deflection of cantilevered elastica compressed by angled cable, *AIAA Journal* 44 (2006) 1468–1476.
[9] T. Sakiyama, A method of analyzing the elastic buckling of tapered columns, *Computers and Structures* 23 (1986) 119–120.
[10] W.G. Smith, Analytic solutions for tapered column buckling, *Computers and Structures* 28 (1988) 677–681.
[11] P.C. Raju, G.V. Rao, Post-buckling analysis of tapered cantilever columns, *Computer Methods in Applied Mechanics and Engineering* 15 (1978) 201–206.
[12] B.K. Lee, S.J. Oh, Elastica and buckling load of simple tapered columns with constant volume, *International Journal of Solids and Structures* 37 (2000) 2507–2518.
[13] V.R. Rajeev, B.P. Madhusudan, B.N. Rao, Post-buckling of cantilever columns having variable cross-section under a combined load, *International Journal of Non-Linear Mechanics* 38 (2003) 1513–1522.
[14] J.B. Salter, Tests on tapered steel columns, *The Structural Engineer* 58A (1980) 189–193.
[15] B.A. Coulter, R.E. Miller, Vibration and buckling of beam–columns subjected to nonuniform axial loads, *International Journal for Numerical Methods in Engineering* 23 (1986) 1739–1755.
[16] K.K. Raju, G.V. Rao, Free vibration behavior of tapered beam columns, *Journal of Engineering Mechanics* 114 (1987) 889–892.
[17] M.J. Maron, *Numerical Analysis: A Practical Approach*, Macmillan, New York, 1982.
[18] D.B. Holland, Static and Dynamic Characteristics of End-Loaded Beams with Specific Application in Square Solar Sails, PhD Dissertation, Duke University, Durham, North Carolina, 2006.